8-1980

A Study of the Target Thickness Effect for Chlorine on Germanium from 25 to 49.5 MeV

James Robert Slusser
Western Michigan University

A STUDY OF THE TARGET THICKNESS EFFECT FOR CHLORINE ON GERMANIUM FROM 25 TO 49.5 MeV

by

James Robert Slusser

A Thesis
Submitted to the
Faculty of The Graduate College
in partial fulfillment of the
requirements for the
Degree of Master of Arts
Department of Physics

Western Michigan University
Kalamazoo, Michigan
August 1980

ACKNOWLEDGEMENTS

I would like to acknowledge the effective and patient guidance of Dr. E. M. Bernstein. Also I wish to thank Dr. M. Soga and Dr. A. Dotson for offering helpful suggestions to the manuscript. Special thanks go to Dr. J. A. Tanis who sent data before its publication and also provided the least squares fitting program used in the analysis of the data. Thanks also to R. Kuhn, who modified the fitting program for WMU's computer, and to the people at the Computer Center who provided time on the system. Finally thanks to Mr. W. Merrow for many helpful discussions concerning this paper.

I would also like to acknowledge research assistantships for the spring and summer of 1979 provided by The Graduate College and by a grant from the Precision Kawasaki Company, Ltd.

James Robert Slusser

TABLE OF CONTENTS

LIST OF TABLES

LIST OF FIGURES

CHAPTER I

INTRODUCTION

Information concerning the electronic structure of atoms may be obtained by observing the effects of high velocity ions colliding with target atoms. Inner shell ionization, the stripping of an atom's most tightly bound electrons, was first investigated by Chadwick in 1912. Using alpha particles from a radioactive source as projectiles, he studied the x-rays emitted from various metal targets. He found that each metal emitted a characteristic x-ray of a given frequency. Mosely (1912) continued this investigation systematically for foils of different atomic number and deduced the well known relationship between the wavelength of the x-ray and the atomic number of the target.

The first theory of inner shell ionization was developed by Henneberg in 1933. This calculation which is called the Plane Wave Born Approximation (PWBA) treated the projectile ion as a point charge which perturbs a bound electron of the target atom via the Coulomb interaction. Both projectile and target atom are treated as plane waves. The PWBA provides a very good description of the observed x-rays resulting from protons and alpha particles incident on a wide range of targets, $15 \leq Z \leq 70$, and over three orders of magnitude of projectile energy (Garcia, Fortner, & Kavanagh, 1973). Modern studies of x-ray production by protons and heavier projectiles began in the early 1950's with the development of scintillation

counters and later solid state, Si(Li), detectors. Lewis, Simmons, and Merzbacher (1953) studied the K-shell x-ray production by protons and Bernstein and Lewis (1954) investigated proton induced L-shell x-ray production. The early work in this field is discussed in the review article by Merzbacher and Lewis (1958).

Larger accelerators and better ion sources have made beams of heavier ions available. X-ray production has been measured using such ions as lithium, carbon, oxygen, sulfur, and all the way to lead (Garcia et al., 1973; Meyerhof, Anholt, Saylor, & Bond, 1975).

Some of the assumptions used in the PWBA are no longer valid for these heavier ions and the observed x-ray production no longer agrees with this theory. Heavy ions bring in complicated electronic structures that interact with target atoms in ways other than simple two body Coulomb forces; thus, the assumption that the projectile may be treated as a point charge is no longer valid.

One model that has been proposed for heavy ion collisions is the quasi-molecular model of Fano and Lichten (1965). If the projectile's velocity relative to the target atom is less than the orbital velocity of the bound electrons, the electrons will be able to adjust to the changing Coulomb field. Energy level diagrams may be computed (Barat & Lichten, 1972) which show how the electron shells overlap with decreasing separation of projectile and target nuclei until at very small distances a "united atom" of $Z = Z_1 + Z_2$ is briefly formed where Z_1 is the nuclear charge of the projectile and Z_2 is the nuclear charge of the target.

In the collision process the electronic structure of the target and projectile atoms may be altered as electrons are given enough energy to move to higher levels or become unbound and leave the atom. The vacancies produced will be filled in one of several ways. An unbound electron may fill the vacancy, or an electron from a higher level may fill the vacancy. In each case the energy that the electron loses as it moves to a lower level will be given up as either an Auger electron or as a photon. An Auger electron is ejected from the atom with an energy equal to the difference between the initial and final binding energy of the transition. Similarly, the photon will have the energy $E = h\nu$ equal to the difference in the energy liberated by filling the vacancy, where h is Planck's Constant and ν is the frequency of the photon.

Experiments by Betz, Bell, Panke, Kalkoffen, Welz, and Evers (1974); Gardner, Gray, Richard, Schmiedekamp, Jamison, and Hall (1977); Gray, Richard, Jamison, and Hall (1976); and Hopkins (1975) indicated that the yield of target and projectile x-rays from various metal foils are not simply proportional to target thickness, or equivalently, that the effective x-ray production cross section varies with target thickness. A model used to describe the variable effective cross section for x-ray production in ion-atom collisions is the two component model of Betz et al. (1974) that was developed to explain the target thickness effect obtained for sulfur ions moving through thin solid targets. In this model it is assumed that the target x-ray cross section for a projectile with a vacancy in the K-shell is larger than the cross section for a projectile without

a K vacancy and that multiple collisions occur within the target allowing a projectile first to collide with a target atom, create a vacancy in its own K shell, and later transfer this vacancy to a target atom in another collision. The projectile vacancy initially created must have a lifetime comparable to the mean free path of the ion divided by the velocity of the ion if it is to transfer this vacancy to a target atom in the second collision. As the projectile moves through the target, vacancies are being filled and vacancies are being created. The two processes must proceed at different rates in order to observe changing target and projectile x-ray cross sections.

For lighter ions such as fluorine and sulfur incident on copper targets, it has been found by Gardner et al. (1977) that the fraction of the beam in the target with two K vacancies has an effect on the x-ray cross section that can not be ignored. In the present work a two component model appears to be suitable for describing the x-ray cross section. The effect of two K vacancies is therefore considered to be negligible.

Feldman, Silverman, and Fortner (1976) used an argon beam incident on thin foils of aluminum and were able to describe the nonlinear target K x-ray cross section by considering the fraction of the beam with an L (2p) shell vacancy as the beam moved through the target. Bernstein and Ferguson (1979) used bromine beams at 55 MeV on germanium and found that the observed target thickness effect could also be described by considering the changing fraction of the beam with L vacancies as the beam moves through the target. In these later cases

the fraction of the projectiles with K shell vacancies is very small and hence do not produce any observable effects.

This work involves measurements of the target thickness effects of a chlorine (Cl) beam on germanium (Ge) targets. The effective target x-ray production cross sections were studied at energies of 25, 30, and 35 MeV. Measurements made by Guiter (1979) at 40 MeV are included in the analysis, as are those of Bernstein (1980), who measured target and projectile x-ray production at 49.5 MeV. Finally measurements were made at 49.5 MeV which utilized beams of several different pure charge states corresponding to different numbers of L shell vacancies. These measurements showed no observable dependence of the x-ray production cross section on the number of L shell vacancies.

The analysis of the data has led to the conclusion that the observed target thickness effect for target and projectile x-ray cross sections for Cl on Ge can be described by a two component model which treats the changing fraction of the beam with one K vacancy as the beam travels through the target. A least squares fit to the data allows the determination of several physical parameters concerning K shell vacancy processes in the projectile atoms.

CHAPTER II

THEORY

The present work involves measurements of the K shell x-rays produced in the collision of chlorine ions incident on thin solid germanium targets. The average effective target x-ray cross section, $\bar{\sigma}_x^t(T)$, which is a function of target thickness, T, is defined by the following relation:

$$\bar{\sigma}_x^t = \frac{Y(T)}{I_0 n \varepsilon} , \qquad (1)$$

where Y(T) is the x-ray yield for target thickness T, I_0 is the number of incident particles, n is the number of target atoms per cm^2, and ε is the detector efficiency for target x-rays.

As noted earlier there are two conditions for observing a target thickness effect, namely a changing fraction of the beam with one K vacancy as the beam moves through the target, and a target x-ray production cross section which is larger for projectiles with one K vacancy than for projectiles with no K vacancies. Thus,

$$\sigma_1^t = \alpha \sigma_0^t \qquad (\alpha > 1),$$

where σ_1^t is the target x-ray cross section for a projectile with a K shell vacancy and σ_0^t is the target x-ray cross section for a projectile without a K shell vacancy.

The differential equation describing the change in K shell vacancies in the beam as it moves through the target is obtained (Gray et al., 1976) as follows: Let $Y_1(x)$ be the fraction of the

beam with one K vacancy at a depth x in the target and $Y_0(x) = 1 - Y_1(x)$ be the fraction of the beam at depth x with no K vacancies. Then

$$\frac{dY_1(x)}{dx} = \sigma_v Y_0(x) - \sigma_d Y_1(x) \tag{2}$$

where σ_v is the projectile K vacancy production cross section and σ_d is the projectile K vacancy decay cross section including all modes of filling the vacancies. Then

$$\frac{dY_1(x)}{dx} = \sigma_v(1 - Y_1) - \sigma_d Y_1$$

or

$$\frac{dY_1(x)}{dx} = \sigma_v - \sigma Y_1, \text{ where } \sigma = \sigma_d + \sigma_v$$

The solution to this equation is:

$$Y_1(x) = \frac{\sigma_v}{\sigma}\ (1 - e^{-\sigma x}) \quad + Ae^{-\sigma x} \tag{3}$$

where A is the fraction of the beam entering the target with one K vacancy.

The effective cross section σ_x^t is the sum of the two cross sections weighted with the fraction of the projectiles in each state:

$$\sigma_x^t = \sigma_0^t Y_0(x) + \sigma_1^t Y_1(x)$$

$$\sigma_x^t = \sigma_0^t[1 - Y_1(x)] + \alpha\sigma_0^t Y_1(x)$$

$$\sigma_x^t = \sigma_0^t[1 + (\alpha - 1)Y_1(x)].$$

To find the average cross section for a target of thickness T, $\bar{\sigma}_x^t(T)$, integrate σ_x^t from x = 0 to x = T and divide by T.

$$\bar{\sigma}_x^t(T) = \frac{\sigma_0^t}{T} \int_0^T [1 + (\alpha - 1)Y_1(x)]dx$$

$$\bar{\sigma}_x^t(T) = \sigma_0^t[1 + (\alpha - 1)\frac{\sigma_v}{\sigma} + (\alpha - 1)\frac{\sigma_v}{\sigma} - A \quad (\frac{e^{-\sigma T} - 1}{\sigma T})] \quad (4)$$

The parameter α may be determined experimentally by taking the ratio of the target x-ray cross section for a vanishingly thin target of a beam composed entirely of projectiles with one K vacancy to that of a beam with no K vacancies (Gardner et al., 1977; Tanis & Shafroth, 1978). Gray et al. (1976) suggest that α may be related to direct charge transfer. A target K vacancy is created by transferring a target K electron to the projectile. In this formulation,

$$\alpha - 1 = \frac{\omega w \pi R^2}{\sigma_0^t}, \quad (5)$$

where ω is the fluorescence yield for the target and R is the radius corresponding to the peak in the dynamic coupling element as calculated by Taulbjerg, Vaaben, and Fastrup (1975). The parameter w (Meyerhoff, 1973) is a semi-empirical probability that a vacancy in the K shell of the projectile is transferred to the K shell of the target atom. Experimentally measured values of α compare well with theoretical calculations of α for ions with Z = 9, 13, 14, 16, and 17 incident on copper targets at energies per unit projectile mass of 1.7 MeV/amu (Gardner et al., 1977).

The yield of the projectile x-rays may also be described by using a two component model (Betz et al., 1974; Tanis & Shafroth, 1978). For the projectiles one must consider the x-rays produced inside the target and those produced outside the target. Inside the foil the number of x-rays produced, dN_x^i is

$$dN_x^i = I_0 Y_1(x) \lambda_x \varepsilon' dx \ , \tag{6}$$

where λ_x is the decay probability per unit path length, and ε' is the detection efficiency for projectile x-rays. Then

$$N_x^i(T) = I_0 \lambda_x \varepsilon' \int_0^T Y_1(x) dx \tag{7}$$

Outside the foil the observed x-ray intensity, N_x^0, is

$$N_x^0(T) = I_0 Y_1(T) \omega_K \varepsilon' \ , \tag{8}$$

where T is the target thickness and ω_K is the mean K-shell fluorescence yield of the ionized projectiles. Summing these contributions gives the total projectile x-ray yield:

$$N_x^{tot}(T) = N_x^i + N_x^0 = I_0 \bar{\sigma}_x^p (T) T \varepsilon' \ ,$$

where $\bar{\sigma}_x^p$ is the average effective x-ray cross section.

Using equations (7) and (8), $\bar{\sigma}_x^p$ can be written

$$\bar{\sigma}_x^p(T) = \frac{I_0 \lambda_x \varepsilon' \int_0^T Y_1(x) dx + I_0 Y_1(T) \omega_K \varepsilon'}{I_0 T \varepsilon'} \ . \tag{9}$$

This may be integrated to yield:

$$\bar{\sigma}_x^p(T) = \lambda_x \left[\frac{\sigma_v}{\sigma} - \left(\frac{\sigma_v}{\sigma} - A \right) \left(\frac{1 - e^{-\sigma T}}{\sigma T} \right) \right]$$

$$+ \omega_K \left[\frac{\sigma_v}{\sigma T} (1 - e^{-\sigma T}) + \frac{A}{T} e^{-\sigma T} \right] . \tag{10}$$

CHAPTER III

EXPERIMENTAL SETUP

A beam of negative chlorine ions was obtained by injecting freon gas into a duoplasmatron ion source, then accelerating the negative ions produced through the Western Michigan University EN tandem Van de Graaff accelerator. By gas stripping in the terminal, charge states of 6^+, 7^+, and 8^+ were obtained at energies ranging from 25 MeV to 49.5 MeV. The terminal voltage of the machine ranged from 3.6 MV to 5.5 MV during these runs.

Thin foils of Ge, ranging in thickness from about 1 to 180 $\mu g/cm^2$ were prepared by vacuum evaporation onto thin carbon backings which were 8 $\mu g/cm^2$ or 23 $\mu g/cm^2$ thick. A movable target ladder was used which allowed six targets to be placed in the target chamber and changed after each run. The ladder could rotate on its axis to present a different effective thickness to the beam. Rotating the target by 180° to present the carbon foil to the beam first provided a final stripping of the chlorine beam, resulting in a higher average charge state entering the germanium target. Figure 1 shows a schematic diagram of the target chamber and experimental setup. Target thicknesses were determined by comparison of the particle yields from the targets to the yields from targets whose thicknesses had previously been determined (Bernstein, 1980).

A lithium drifted silicon detector (Si(Li)) placed 4.35 cm below the target at an angle of 90° to the beam detected the germanium

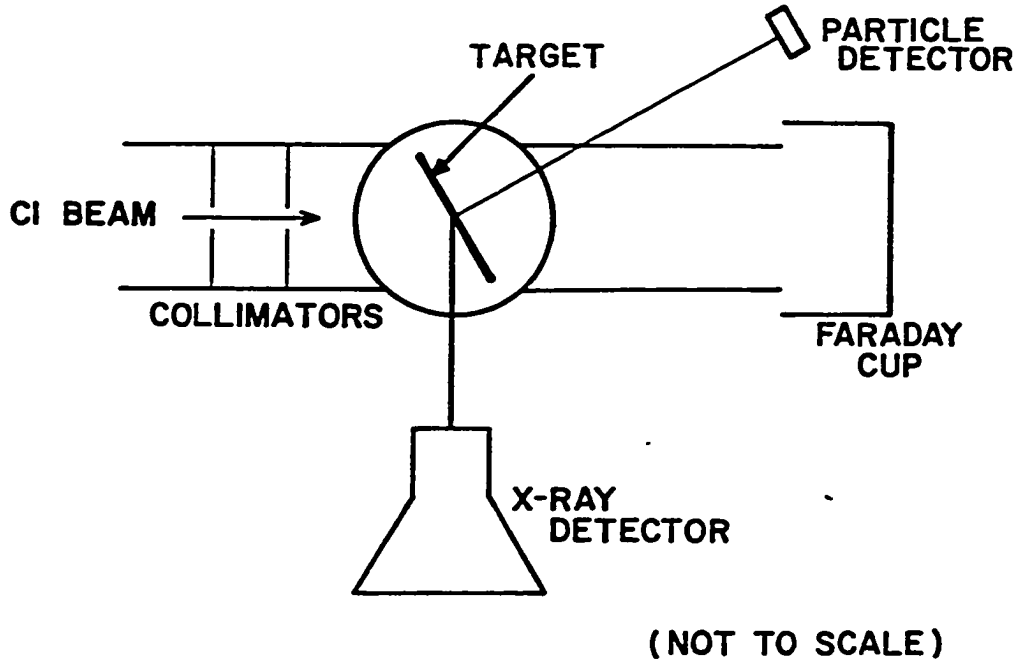

Figure 1. Experimental geometry. The particle detector is at an angle of 30° relative to the beam direction and the x-ray detector is at an angle of 90° relative to the beam direction.

K_α x-rays; particles were detected by a surface barrier detector at an angle of 30° to the beam and 5.99 cm from the target. The system had collimating slits of 0.23 cm diameter and 0.64 cm diameter placed 18.7 cm and 26.4 cm, respectively, in front of the target, and an aluminum absorber 0.00254 cm thick placed between the target and the x-ray detector to attenuate unwanted chlorine x-rays. The signals from the particle and x-ray detectors were sent through preamplifiers near the detectors and then through cables into the control room. The pulses were then amplified and sent to a discriminator and scaled or fed into the computer and stored on magnetic tape. A diagram of the experimental electronics is given in Figure 2.

The system had a provision for reducing "dead time" and x-ray pulse pile-up. "Beam-flipping" plates at 1500 volts (Thibeau, 1973) shunted the beam away from the target each time the detector registered an x-ray pulse. The beam is swept away from the target in less than 0.5 μs and returns to the target within about 50 μs. The dead time correction was made by taking the ratio of the total number of x-rays detected to the total number of x-rays counted and multiplying the yield of germanium K_α x-rays by this factor. A typical x-ray spectrum at 40 MeV is shown in Figure 3.

Runs were made for a specific amount of charge collected in the Faraday cup; the quantity of charge collected ranged from 8×10^{-6} to 4×10^{-4} coulombs.

A carbon foil stripper located after the analyzing magnet allowed stripping to higher charge states than those of the accelerated beams. With this external stripper in place, pure charge states

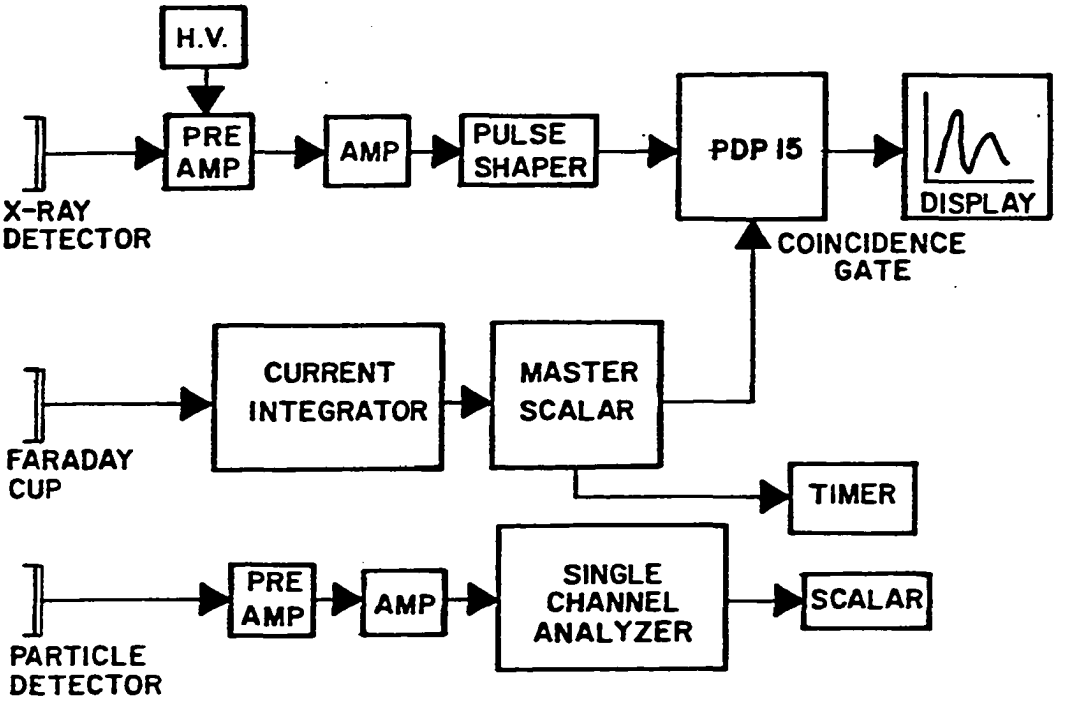

Figure 2. Electronics block diagram.

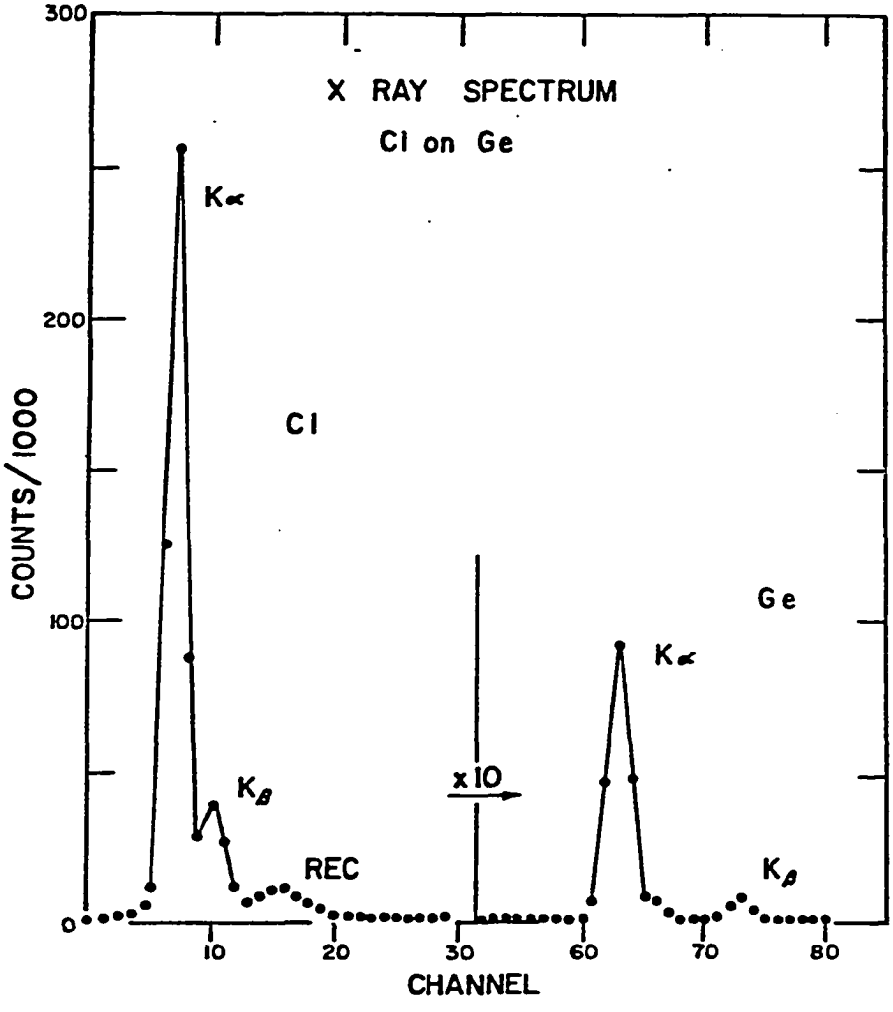

Figure 3. X-ray spectrum from the Si(Li) detector for Cl on Ge at 40 MeV. Note the relative intensities of the Cl K_α and the Ge K_α lines.

were selected by the switching magnet and sent to the target. At 49.5 MeV, charge states of Cl projectiles of 8^+, 10^+, 11^+, 12^+, 13^+, and 14^+ were obtained, corresponding to 1, 3, 4, 5, 6, and 7 L shell vacancies. Figure 4 shows the results of measurements of x-ray cross sections for Ge targets of 6 $\mu g/cm^2$ and 32 $\mu g/cm^2$ vs. charge state, q, of the incident ion. Within the uncertainties there is no change in the target x-ray cross section for projectiles with different numbers of L vacancies. This provides strong evidence that the observed target thickness effects in this case are due to K vacancies.

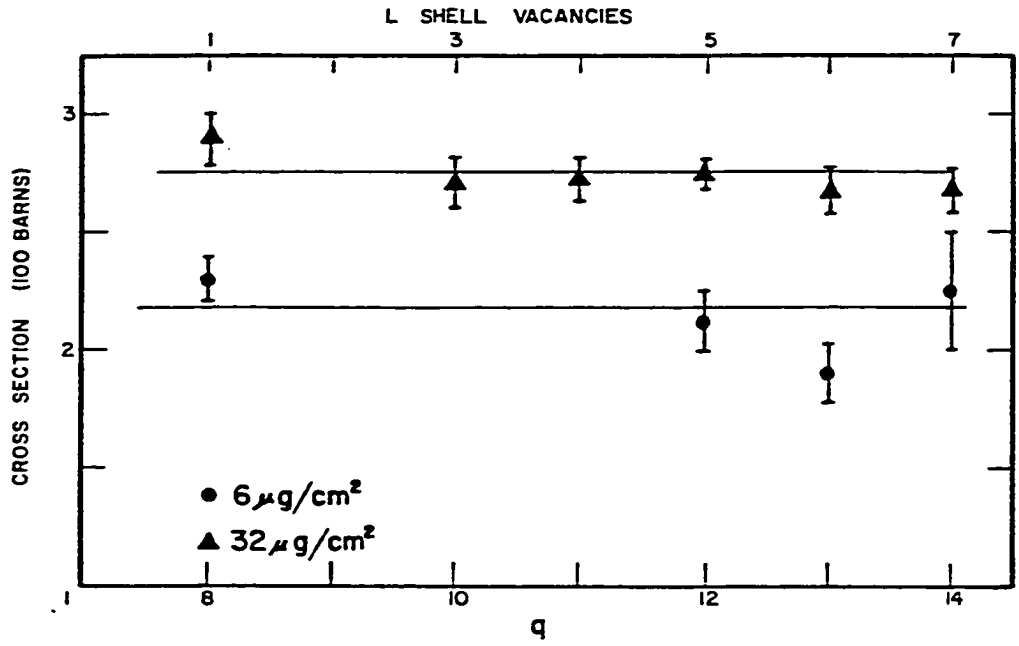

Figure 4. Target x-ray cross section vs. charge state, q, of the incident ions. The number of L vacancies is shown on the top scale and q is shown on the bottom scale. The solid straight line is the average value for all q. The solid circles are cross sections for T = 6 μg/cm^2 and the solid triangles are cross sections for T = 32 μg/cm^2.

CHAPTER IV

DATA ANALYSIS

After each run the target number, target thickness, angle of the target to the beam, current integration count, time of run, particle count, and germanium K_α x-ray yield corrected for dead time were recorded. For a particular target at a given target angle, current integration counts, particle counts, and germanium K_α x-rays were totaled. A background correction was made by counting the number of x-rays that resulted in passing the beam through a carbon foil of the same thickness as the target backings.

The ratio of germanium x-rays to scattered particles is used to determine the effective target x-ray production cross section. The particle count is used instead of a charge integration because of the difficulty for heavy ions in accurately determining the number of incident particles from the collected charge. With the thin targets used, the scattering of projectiles is very well described by the Rutherford formula. The yield of x-rays, Y_X, is:

$$Y_X = I_0 \bar{\sigma}_X T \frac{d\Omega_X}{4\pi} \varepsilon_X ,$$

where I_0 is the number of particles in the beam, T is the target thickness, $d\Omega_X$ is the solid angle subtended by the x-ray detector, and ε_X is the efficiency of the x-ray detector. The particle yield, Y_p, is:

$$Y_p = I_0 \left(\frac{d\sigma}{d\Omega}\right)_{R,LAB} T d\Omega_p ,$$

where $\left(\frac{d\sigma}{d\Omega}\right)_{R,LAB}$ is the Rutherford scattering cross section in lab coordinates and $d\Omega_p$ is the solid angle of the particle detector. The particle yield includes germanium recoils as well as scattered chlorine projectiles, both detected at an angle of 30° in the laboratory relative to the beam. To calculate the cross section for germanium recoils it can be shown that for germanium to scatter at 30° in the lab, chlorine must scatter at 120° in the center of mass frame.

Corrections for the energy loss as the beam traveled through the target were made by using values of the electronic stopping power of germanium and carbon (Northcliffe & Schilling, 1970). All results are corrected to the same energy at the center of the target. For targets with germanium first, $\frac{\Delta E_{Ge}}{2}$ is the energy loss to the center of the target. For the runs where the beam first went through the carbon backing, the beam lost energy through the carbon as well as the germanium; the total energy loss was $\Delta E' = \frac{\Delta E_{Ge}}{2} + \Delta E_C$ where ΔE_C is the energy loss in carbon. This energy loss affects the particle yield because the Rutherford cross section varies as E^{-2}. The x-ray yield varies as $E^{5.38}$ in the energy range of interest. This energy dependence for the x-rays was determined by graphing the x-ray yield vs. energy at 30, 35, 48.5, 49.0, and 49.5 MeV on semi-log paper. The effective x-ray cross section $\bar{\sigma}_x$, which is proportional to Y_x/Y_p, is therefore proportional to $E^{7.38}$. For

$$\bar{\sigma}_x = kE^m$$

Then

$$d\bar{\sigma}_x = mkE^{m-1}dE \ ,$$

and

$$\frac{d\bar{\sigma}_X}{\sigma_X} = m \frac{dE}{E} .$$

Thus, the correction factor for target x-rays for the germanium first points was $Y_X \left[1 + 7.38\frac{\Delta E_{Ge}}{2E}\right]$, and for the carbon first points $Y_X \left[1 + 7.38 \left(\frac{\Delta E_{Ge}}{2E} + \frac{\Delta E_C}{E}\right)\right]$. The combined corrections ranged from less than 1% to as much as 17% for the thickest targets with carbon first.

Windows were set so that only the germanium K_α x-rays were counted. The target x-ray yield was multiplied by 1.169 to account for the germanium K_β x-rays. This factor was obtained at 49.5 MeV (Bernstein, 1980).

There are two major sources of uncertainty in the relative x-ray production cross sections. These uncertainties are: statistical fluctuations which give an uncertainty of $\Delta N = N^{\frac{1}{2}}$ for N counts, and the uncertainty connected with the reproducibility of the data which is presumably caused by changes in the position of the beam and by target nonuniformities. The statistical uncertainties ranged from less than 1% to about 5%, while reproducibility errors were assigned an estimated value of 3%. The overall uncertainties in the relative cross sections were almost always smaller than 4%.

The uncertainties in the absolute target x-ray production cross sections are estimated to be about ±20%, while the uncertainties in the absolute projectile x-ray cross sections are estimated to be ±30%. These uncertainties in the absolute cross sections are similar

in magnitude to other measurements (Garcia et al., 1973). Since the quantities of primary interest in this work are determined by the relative cross sections, the magnitudes of the uncertainties in the absolute cross sections are acceptable.

CHAPTER V

RESULTS AND DISCUSSION

Target X-ray Cross Sections

If projectiles with only a single value of A are available, for example a beam entering the target with no K vacancies (A = 0), a least squares fit to Equation (4) allows determination of σ_0^t, σ, and the product $\sigma_V(\alpha - 1)$. The quantities σ_V and $(\alpha - 1)$ can be determined independently if projectiles with two different known values (Gray et al., 1976) of A (e.g. A = 0 and A = 1) are available. In the present work nonzero values of A were obtained by passing the beam through the carbon target backing first. When the results obtained with a beam of nonzero (but unknown) A are fit to Equation (4) simultaneously with the results obtained with a beam with A = 0, the product $(\alpha - 1)A$ is determined in addition to the other three parameters which are common to both sets of data. Table 1 and Table 2 show the results obtained using a least squares fitting computer program developed by Tanis (1979). The values of the parameters for the A = 0 data are shown in Table 1, and the values for the simultaneous fits for beams with nonzero A values and zero A values are shown in Table 2. The errors quoted are only the "fitting errors" from the least squares analysis. These fitting errors were obtained by determining approximately the values of the parameters which gave an average error per data point about 20% to 30% larger than

Table 1

Least Squares Fit Parameters for Ge First Data

E (MeV)	σ_0^t (b)	$(\alpha - 1)\sigma_v$ (1000 Kb)	σ (1000 Kb)
25	$5.1^{+0.6}_{-0.2}$	$6.2^{+3.5}_{-1.7}$	$17.9^{+7.6}_{-1.9}$
30	$12.7^{+0.1}_{-0.3}$	$8.4^{+1.5}_{-0.6}$	$22.8^{+5.6}_{-1.7}$
35	$26.1^{+0.9}_{-0.1}$	$11.3^{+0.8}_{-2.8}$	$19.2^{+1.3}_{-2.6}$
40	$58.4^{+2.0}_{-0.1}$	$11.1^{+1.4}_{-3.0}$	$15.1^{+1.9}_{-3.8}$

Table 2

Least Squares Fit Parameters for Ge First and C First Data Combined

E (MeV)	σ_0^t (b)	$(\alpha - 1)\sigma_v$ (1000 Kb)	σ (1000 Kb)	$A(\alpha - 1)$
30	$12.9^{+0.1}_{-0.3}$	$6.0^{+1.9}_{-2.4}$	$16.6^{+3.6}_{-0.6}$	$0.470^{+0.08}_{-0.01}$
35	$27.1^{+0.4}_{-0.1}$	$7.5^{+2.6}_{-1.0}$	$11.8^{+3.4}_{-1.2}$	$0.724^{+0.08}_{-0.01}$
40	$58.2^{+0.1}_{-0.2}$	$11.2^{+0.8}_{-1.2}$	$15.0^{+1.2}_{-1.6}$	$0.532^{+0.01}_{-0.02}$
49.5[a]	$191.1^{+5.8}_{-4.7}$	$6.4^{+0.56}_{-0.13}$	$7.1^{+0.3}_{-1.2}$	$0.655^{+0.7}_{-0.3}$

[a]At this energy projectile data was also fit in the least squares analysis.

the error per point for the best fit parameters. The parameters determined at 49.5 MeV were obtained by fitting projectile x-ray cross sections simultaneously with the A = 0 and A ≠ 0 cross sections. Figure 5 shows target x-ray cross sections vs. target thickness for E = 25, 30, 35, and 40 MeV along with the two component model fits. Figure 6 shows the target x-ray cross section at 49.5 MeV as well as the projectile x-ray yield (see below) at this energy along with the fits.

If a determination of A can be made, α may be calculated from the value of $(\alpha - 1)A$. Values of A can be determined for a given thickness of carbon (C) using Equation (3) if σ and σ_V are known for Cl on C. The thicknesses of the carbon backings used in this experiment were 27.5 $\mu g/cm^2$ at 25, 30, and 35 MeV and 9.5 $\mu g/cm^2$ at 40 and 49.5 MeV.

Tanis, Shafroth, and Willis (1979) have made measurements of σ and the vacancy production cross section, σ_V, for Cl on C at energies of 40, 60, and 80 MeV. In the determination of σ_V, Tanis et al. (1979) made use of Cl on Cu data. In the present analysis the Cl on Cu data has been recomputed using a different value of R in Equation (5). The value in atomic units (a.u.) used was R = 2.85 a.u./$(Z_2 - 3/4)$ (Taulbjerg et al., 1975) instead of R = 2.6 a.u./Z_2 given by Gray et al. (1976). It is not clear how Gray et al. arrived at their value for R since it was also obtained from Taulbjerg et al. (1975). Using the recomputed values of σ_V for Cl on C and values interpolated and extrapolated from these values on a log-log graph, A has been determined at the energies of interest. The values of A are given in column 4 of Table 3.

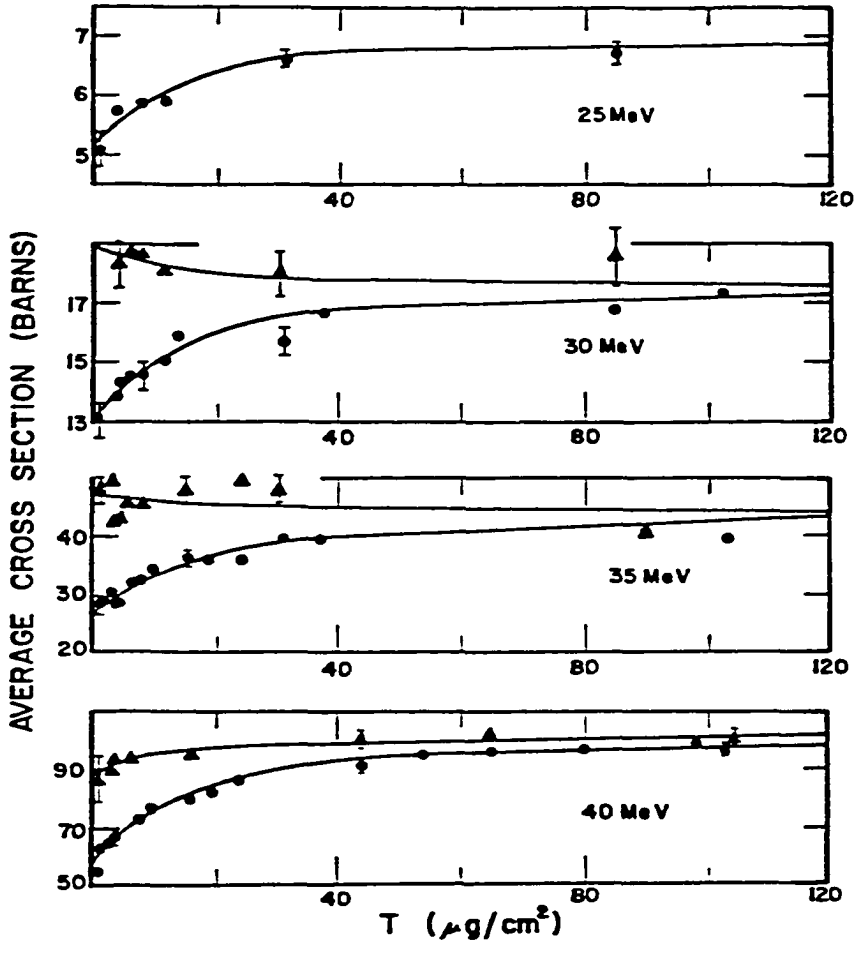

Figure 5. Target K x-ray production cross sections vs. target thickness for Cl on Ge at 25, 30, 35, and 40 MeV. The solid circles are for data points with A = 0, and the solid triangles are for points with A ≠ 0. The solid curves are least squares fits to the data.

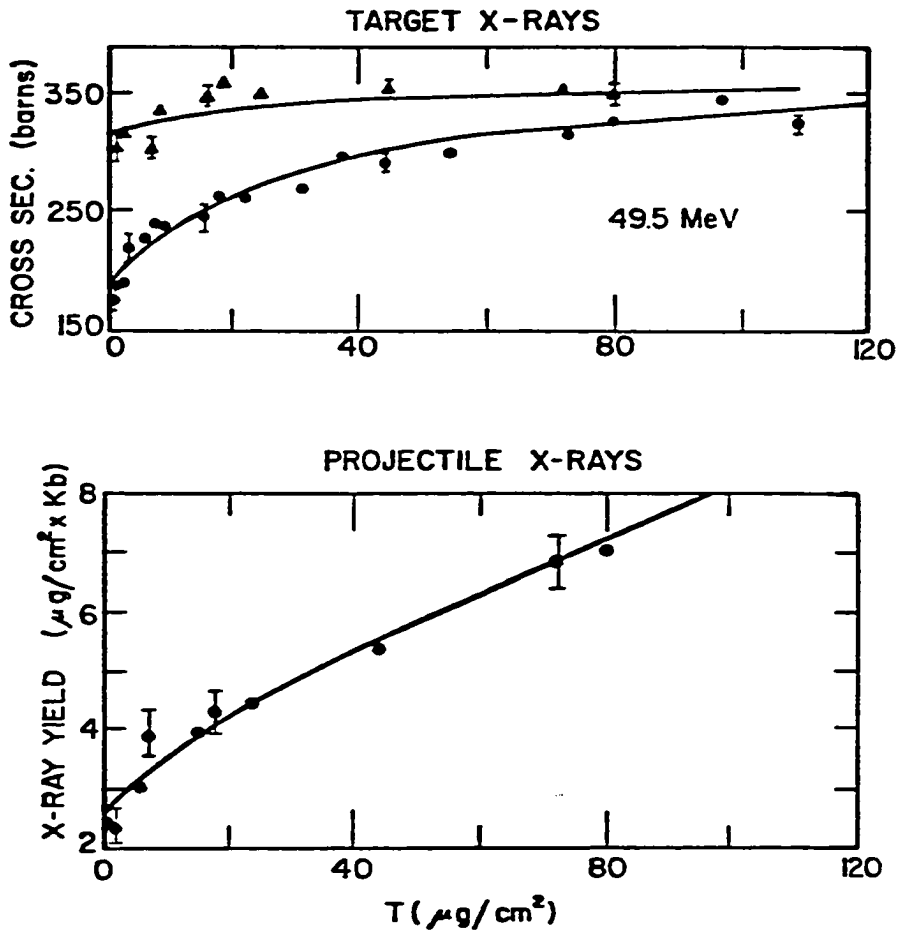

Figure 6. At the top is shown the target K x-ray production cross section vs. target thickness for Cl on Ge at 49.5 MeV. Solid circles are for A = 0 and solid triangles are for A ≠ 0. The solid curves are the least squares fits to all the data at this energy. At the bottom is shown the projectile K x-ray yield vs. target thickness for Cl on Ge at 49.5 MeV. The yield is given in terms of the cross section in kilobarns times the target thickness in $\mu g/cm^2$. The solid curve is the result of the least squares fit to all the data at this energy.

Table 3

Comparison of Experimental and Theoretical Values of α

E (MeV)	α (Theory)[a]	α (Exp.)[b]	A[c]	σ_v[d] (Kb)	σ_v[e] (Kb)
30	38.9	35.8	0.0135	158^{+50}_{-64}	172^{+55}_{-69}
35	30.2	34.5	0.0216	258^{+89}_{-34}	224^{+78}_{-30}
40	21.0	21.5	0.0259	560^{+40}_{-60}	546^{+39}_{-59}
49.5	11.8	12.9	0.0551	593^{+52}_{-12}	538^{+47}_{-11}

[a]Calculated using Equation (5).

[b]Obtained from value of A in column 4 and $(\alpha - 1)A$ value given in Table 2.

[c]From Cl on C measurements.

[d]Calculated from $(\alpha - 1)\sigma_v$ in Table 2 using the value of α from column 2.

[e]Calculated from $(\alpha - 1)\sigma_v$ in Table 2 using the value of α from column 3.

In Table 3 the values of α obtained using the values of A calculated from the C data and the $(\alpha - 1)A$ values from the least squares fit are compared to the values of α found using Equation (5). The value of R used in the calculation for Cl on Ge was R = 2.6 a.u./$(Z_2 - 3/4)$, where Z_2 is the atomic number of Ge, 32. This value for R was extrapolated from the calculations given in Taulbjerg et al. (1975) and is consistent with the value of R used for Cl on Cu. The

value of ω is 0.540 (Bambynek, Crasemann, Fink, Freund, Mark, Swift, Price, and Rao (1972). The He-like binding energy of Cl, 3.6584 keV (Kelly & Harrison, 1973) was used in the calculation of the Meyerhoff parameter w. The value of σ_0^t was taken from the least squares fit of A = 0 and A ≠ 0 data. The values of α calculated using the C data agree to within ±15% of the values of α predicted by Equation (5). Using the values of $(\alpha - 1)$ and the $(\alpha - 1)\sigma_V$ values from Table 2, the values of the vacancy production cross section, σ_V, obtained from the two different values of α, are also compared in Table 3. The $(\alpha - 1)\sigma_V$ values come from the simultaneous least squares fit of the A = 0 and A ≠ 0 data.

A plot of σ vs. energy is shown in Figure 7. The large fitting error for 25 MeV indicates that more data needs to be taken at this energy. Because there are so few data points at 25 MeV with carbon first, no attempt was made to simultaneously fit the nonzero A data with the A = 0 data. Values of σ from the fits using the A = 0 data and the combined A = 0 and A ≠ 0 data are slightly offset from the values of σ found using only the A = 0 data. Total cross sections for Cl on Cu (Tanis, Jacobs, & Shafroth, 1980) and Cl on C (Tanis et al., 1979) are shown for comparison. The values of σ for Cl on Ge decline steeply with increasing energy, following the general trend of the other two curves. This occurs because the vacancy decay cross section, which is primarily due to electron capture, decreases with increasing energy more rapidly than the vacancy production cross section increases. As noted earlier σ is the sum of the vacancy

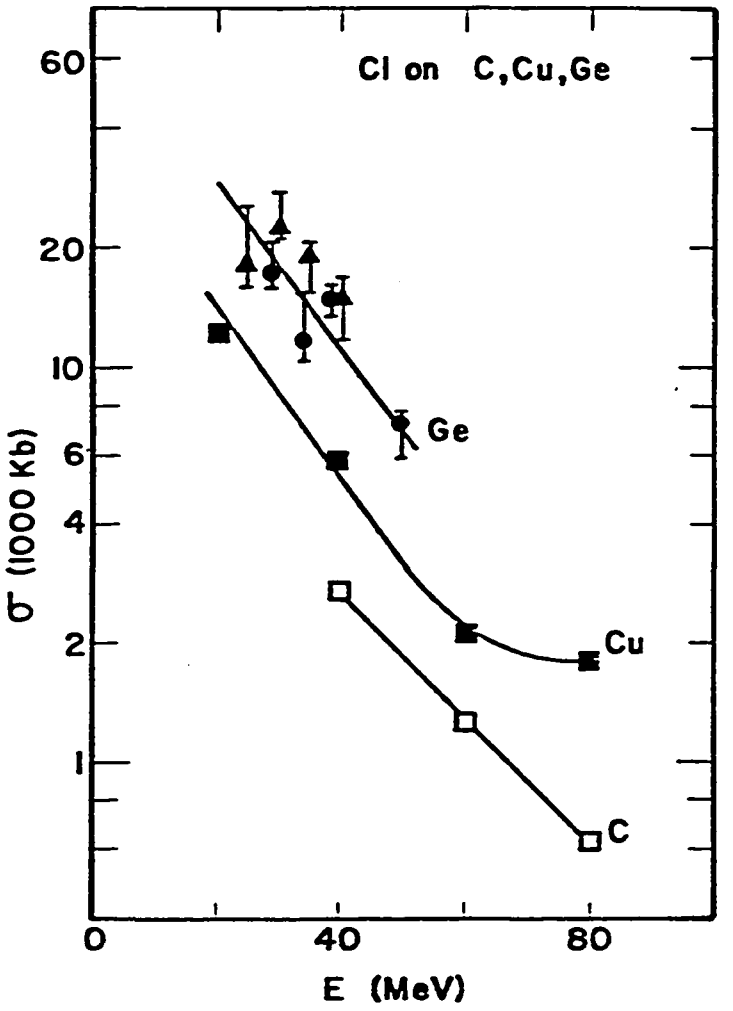

Figure 7. Cross section σ vs. energy for Cl on C, Cu, and Ge. The solid circles represent values of σ for Cl on Ge using both A = 0 and A ≠ 0 data, while the solid triangles are values of σ for Cl on Ge using the A = 0 data only. The solid squares are σ values for Cl on Cu (Tanis et al., 1980) and the open squares are σ values for Cl on C (Tanis et al., 1979). The solid lines are drawn through the points to guide the eye. Error bars show fitting errors only.

production cross sections and the vacancy decay cross sections including all modes of filling K vacancies in the projectile.

Figure 8 is a graph of the vacancy production cross section σ_v vs. energy for Cl on Ge with σ_v for Cl on Cu (Tanis et al., 1980) and Cl on C (Tanis et al., 1979) included for comparison. The vacancy production cross section is seen to increase with energy, reflecting the fact that creating a target K vacancy is more likely for projectiles of higher velocity. From these results it appears that the Cl on Ge values have a somewhat steeper rise with energy than the other two sets of cross sections.

Projectile X-ray Cross Sections

The projectile K x-ray production cross sections measured at 49.5 MeV (Bernstein, 1980) were fit simultaneously with the target x-ray cross sections. A least squares fit to the data determined $\bar{\sigma}_0^p$, the projectile x-ray cross section for zero thickness, the product $\lambda_x\sigma_v$ where λ_x is the radiative decay probability per unit path length, the product $\lambda_x A$, as well as σ_0^t, $(\alpha - 1)\sigma_v$, and σ. The results of the analysis along with the fitting errors are: $\sigma_0^p = 214\ ^{+16}_{-43}$ Kb, $\lambda_x\sigma_v = (354\ ^{+\ 38}_{-113}) \times 10^3$ Kb^2, and $\lambda_x A = 36.2\ ^{+\ 5.8}_{-12.2}$ Kb. Using the value for A from Table 3 column 4 allows determination of $\lambda_x = 657$ Kb.

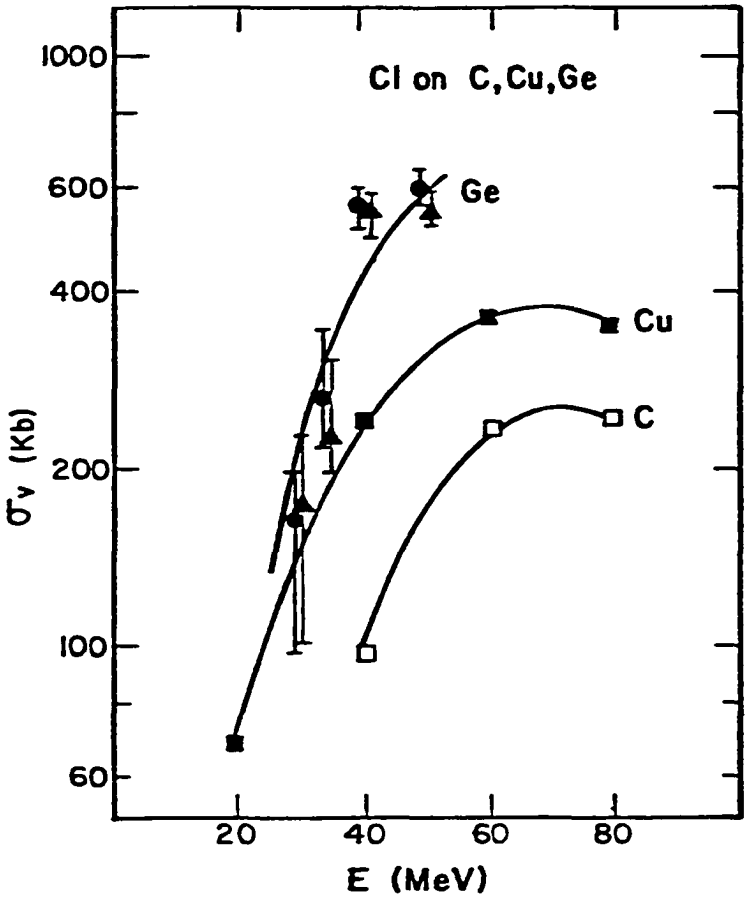

Figure 8. Vacancy production cross section, σ_V, for Cl on C, Cu, and Ge vs. energy. The solid circles represent values of σ_V for Cl on Ge found using the theoretical values of α, while the solid triangles are values of σ_V obtained using the experimental values of α. The solid squares are for Cl on Cu (Tanis et al., 1980) and the open squares are for Cl on C (Tanis et al., 1979). The solid lines are drawn through the points to guide the eye. Error bars show fitting errors only.

CHAPTER VI

CONCLUSIONS

The target thickness dependence of all of the target and projectile K x-ray production cross sections were fit reasonably well using the two component model of Betz et al. (1974). Target x-ray cross sections were enhanced when the beam was passed through the carbon backing first before entering the target. This enhancement can be explained by considering that a certain fraction of the beam emerges from the carbon backing with K vacancies. The target x-ray cross section was found to be independent of the number of L vacancies in the projectiles in agreement with earlier work by Gray et al. (1976) for Cl incident on Cu. This provides strong evidence that the observed target thickness effect for the K x-ray cross sections for Cl on Ge results from K vacancies in the beam.

There is good agreement in the experimentally determined values of α and theoretical values of α, indicating the usefulness of the Gray et al. (1976) formula in the energy ranges of the collision system studied. In addition to fitting the data, the two component model yielded two parameters of physical significance, σ and σ_v, which describe some of the dynamics of the projectile interaction with the target atoms. The energy dependence of σ and σ_v was studied and compared with Cl on C and Cl on Cu. More work is needed at lower energies where the data was limited, and at higher beam energies, especially using higher beam charge states so that beams with A = 1

can be accelerated, and more precise experimental determinations of α made.

BIBLIOGRAPHY

Anholt, R., & Meyerhoff, W. E. K vacancy production in heavy-ion collisions. III. 1s σ excitation. Physical Review A, 1977, 16, 190-208.

Bambynek, W., Crasemann, B., Fink, R. W., Freund, H.-U., Mark, H., Swift, C. D., Price, R. E., & Rao, P. V. X-ray fluorescence yields, Auger, and Coster-Kronig transition probabilites. Reviews of Modern Physics, 1972, 44, 716-813.

Barat, M., & Lichten, W. Extension of the electron promotion model to asymmetric atomic collisions. Physical Review A, 1972, 6, 211-229.

Bernstein, E. M. Personal communication, 1980.

Bernstein, E. M., & Ferguson, S. M. Target thickness dependence of K x-ray production for 55 MeV Br ions in Ge. IEEE Transactions of Nuclear Science, 1978, NS-26, 1133-1136.

Bernstein, E. M., & Lewis, H. W. L-shell ionization by protons of 1.5- to 4.25-MeV energy. Physical Review, 1954, 95, 83-86.

Betz, H.-D., Bell, F., Panke, H., Kalkoffen, G., Welz, M., & Evers, D. New technique for the measurement of lifetimes of heavy-ion inner shell vacancies. Physical Review Letters, 1974, 33, 807-810.

Chadwick, J. The γ rays excited by the β rays of radium. Philosophical Magazine, 1912, 24, 594-600.

Fano, U., & Lichten, W. Interpretation of Ar^{+}-Ar collisions at 50 keV. Physical Review Letters, 1965, 14, 627-629.

Feldman, K. C., Silverman, P. J., & Fortner, R. J. Lifetime studies of Ar-2p-vacancies traveling through solids. Nuclear Instruments and Methods, 1976, 132, 29-33.

Garcia, J. D., Fortner, R. J., & Kavanagh, T. M. Inner-shell vacancy production in ion-atom collisions. Review of Modern Physics, 1973, 45, 111-176.

Gardner, R. K., Gray, T., Richard, P., Schmiedekamp, C., Jamison, K. A., & Hall, J. M. Target thickness dependence of Cu K x-ray production for ions moving in thin solid Cu targets. Physical Review A, 1977, 15, 2202-2211.

Gray, T., Richard, P., Jamison, K. A., & Hall, J. M. Role of residual K-shell vacancies in solid target x-ray cross sections. Physical Review A, 1976, 14, 1333-1337.

Groeneveld, K. O., Kolb, B., Schader, J., & Sevier, K. D. Total K-vacancy production in Ne (10 MeV) transversing Al. Zeitschrift für Physik A, 1976, 277, 13-18.

Guiter, S. Thickness effects on x-ray yields per particle in 40 MeV Cl on Ge collisions. Unpublished senior Honors College paper, Western Michigan University, 1979.

Henneberg, W. Anregung von atomen in inniren schalen durch langsame protenen und α-teilchen. Zeitschrift für Physik, 1933, 86, 592-604.

Hopkins, F. Evidence for residual K-shell excitation in chlorine ions penetrating carbon. Physical Review Letters, 1975, 35, 270-274.

Kelly, R. L., & Harrison, D. E. Ionization potentials, experimental and theoretical, of the elements hydrogen to krypton. Atomic Data, 1973, 3, 177-193.

Lewis, H. W., Simmons, B. E., & Merzbacher, E. Production of characteristic x-rays by protons of 1.7- to 3-MeV energy. Physical Review, 1953, 91, 943-946.

Merzbacher, E., & Lewis, H. W. X-ray production by heavy charged particles. In S. Flugge (Ed.), Handbuch der physik (Vol. 34). Berlin: Springer-Verlag, 1958.

Meyerhoff, W. E. K-vacancy sharing in near-symmetric heavy-ion collisions. Physical Review Letters, 1973, 31, 1341-1344.

Meyerhoff, W. E., Anholt, R., & Saylor, T. K. K-vacancy production in heavy-ion collisions. II. Multiple- and single-collision excitation in the 2pσ molecular orbital. Physical Review A, 1977, 16, 169-189.

Meyerhoff, W. E., Anholt, R., Saylor, T. K., & Bond, P. D. K x-ray yield from 100 MeV Pb + Pb collisions. Physical Review A, 1975, 11, 1083-1085.

Meyerhoff, W. E., Anholt, R., Saylor, T. K., Lazarus, S. M., Little, A., & Chase, L. F., Jr. K-vacancy production in heavy-ion collisions. I. Experimental results for $Z \geq 35$ projectiles. Physical Review A, 1976, 14, 1653-1661.

Mosely, H. G. The high frequency spectra of the elements. Philosophical Magazine, 1913, 26, 1024-1034.

Northcliffe, L. C., & Schilling, R. F. Range and stopping-power tables for heavy ions. Nuclear Data Tables, 1970, A7, 233-463.

Schmiedekamp, A., Gray, T., Doyle, B. L., & Schibel, U. Target and projectile cross sections for F ions on Ti, V, Cr, Fe, and Co: 1.7 MeV/amu. Physical Review A, 1979, 19, 2167-2172.

Tanis, J. A. Personal communication, 1979.

Tanis, J. A., Jacobs, W. W., & Shafroth, S. M. Systematics of target and projectile K x-ray production and REC for 20-80 MeV Cl^{q+} ions incident on 25-200 $\mu g/cm^2$ Cu targets. To be published in Physical Review A, July, 1980.

Tanis, J. A., & Shafroth, S. M. Target thickness dependence of radiative electron capture in heavy-ion collisions. Physical Review Letters, 1978, 40, 1174-1177.

Tanis, J. A., Shafroth, S. M., & Willis, J. Projectile K x-rays and REC from Cl ions incident on carbon foils. Bulletin of the American Physical Society, 1979, 24, 582.

Taulbjerg, K., Vaaben, J., & Fastrup, B. Molecular-orbital theory for K-vacancy sharing in atomic collisions. Physical Review A, 1975, 12, 2325-2332.

Thibeau, H., Stadel, H., Cline, W., & Cahill, T. A. On-demand beam pulsing for an accelerator. Nuclear Instruments and Methods, 1973, 111, 615-617.